Development of a Simplified Analytical Model for a Passive Inertial System Solicited by Wave Motion

**G. Rinaldi[a], A. Fontanella[a], G. Sannino[a], G. Bracco[b],
E. Giorcelli[b], G. Mattiazzo[b], H. Bludszuweit[c]**

[a] ENEA - Italian National Agency for New Technologies, Energy and Sustainable Economic Development, Via Anguillarese 301 Santa Maria di Galera (Roma), Italy.

[b] Department of Mechanical and Aerospace Engineering - Politecnico di Torino, C. Duca degli Abruzzi 24, 10129 Torino, Italy.

[c] Research Centre for Energy Resources and Consumption (CIRCE), C/ Mariano Esquillor Gómez 15, 50018 Zaragoza, Spain.

Abstract: This paper presents a theoretical and experimental investigation about the modelling of a 1:45 scale prototype Wave Energy Converter (WEC). An analytical model is implemented to describe its behaviour in a wave tank. The aim is to provide a contribution to modelling tools used for WEC characterization and design. Hydrodynamic characterization software is avoided in favour of a simpler and more versatile design tool destined to a wider range of users. Therefore, an alternative approach is presented, based on mechanical analogies and the use of Matlab/Simulink/SimMechanics environment. This analytical model was constructed using linear wave theory, coupled with a non-linear model for the device and its power take-off system (PTO). Assumptions on incident waves and geometric properties of the device were required and implemented on the basis of literature of naval architecture, ships stabilization and control issues. Simulation results were compared and validated with those obtained in the same range of experimental tests of the prototype in wave tank. Trends and values of both investigation techniques show a good agreement, indicating the validity of the methodology adopted and leaving space for future improvements of the same. Finally, as example of application, the model was applied in a show case in order to estimate the energy yield by the WEC if scaled to real size, using Froude scaling. Results are encouraging and show the viability of the proposed design.

Keywords: Modelling, Wave Energy Converters (WECs), Inertial Passive Systems, SimMechanics, Froude Scaling, Wave Tank Testing.

1. INTRODUCTION

Ocean energy is acquiring an increasingly important role within the Renewable Energy scenarios. A huge worldwide potential has been recognised for this kind of renewable source [1]. Oceans, in fact, cover approximately 70% of Earth's surface, and it is undeniable that Marine Energy could give an important contribution in a future decarbonized energy mix. The possibility to produce electricity from the sea is not a new topic. However, nowadays it is attracting more and more attention from academic and industrial sectors for being a clean energy source and for the need to boost the economy by creating new promising productive sectors [1]. Energy from the seas can be produced taking advantage of waves, tides, currents, temperature gradient and salinity gradient. Among these sources waves are surely the most tangible form to imagine the sea potential, and probably also for this reason one of the most investigated resources in the Marine Energy sector. Several concept devices, based on different working principles, have been studied and developed to exploit wave energy [2,3]. Basically three main categories exist for wave energy conversion purposes: oscillating water columns (OWC), overtopping systems (OTS), and oscillating body systems (OB). The first category exploits the air pressure oscillations caused by water rise and fall due to incident waves, while Overtopping Systems capture sea water in a reservoir above the sea level and then constrain it to flow through low-head turbines before to be released again to the sea. This work is focused on a converter belonging to the third mentioned category, the Oscillating Body Systems. These devices extract power from waves using a power take-off system (PTO) that is activated taking advantage of the relative movement between two different parts of their structure which oscillate in response to incident waves. Therefore, this kind of devices is called *inertial*, since the inertial motion of a mass respect to a reference frame is used to generate electricity. Typically the functioning of those converters relies on the employment of a rotating and/or a translating mass, or alternatively a gyroscope. Although the operation principle is the same in both cases, an important difference exists between the two choices. In fact, gyroscopic systems require that part of the energy produced by the device is used to maintain the gyroscope itself in rotation for control and optimization purposes [4], which consequently makes the device an *active system*. On the other hand, simple rotating and/or

translating masses do not need energy to react to external solicitations, and are therefore *passive systems*. As a consequence, all the energy absorbed can be converted into electricity (within the limits of energy conversion efficiencies) because there is no need to use a part of the energy produced to feed the device itself. Currently several examples of inertial WECs exist and are employed [4–8]. In order to contribute to their development, and more in general to the entire Marine Energy sector, this paper focuses on the modelling work of a passive inertial Pendulum Wave Energy Converter (named "PeWEC"), developed and currently under investigation within a partnership agreement between ENEA (Italian National Agency for New Technologies, Energy and Sustainable Economic Development) and the Politecnico di Torino University (Italy). Finally, a preliminary estimate of expected energy production in the Mediterranean Sea is performed for a full-scale device.

2. SYSTEM MODELLING

This section presents the experimental and theoretical premises that have been considered in order to investigate the device and create a proper model. The system studied, tested and modelled in this work can be idealized as half-cylindrical hull able to oscillate in pitch in response to wave motion. In its interior it contains a pendulum system, able to swing in one degree of freedom, which in turn is connected to an electric generator. The oscillation of the hull caused by the incident waves is transmitted to the internal pendulum. Hence, the relative motion between hull and pendulum activates a PTO system that produces electricity. Drawings of the hull and the PTO system are represented in Fig. 1.
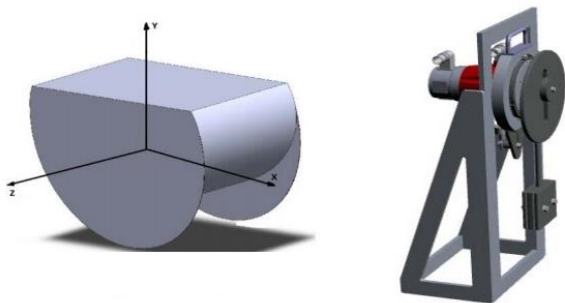

Figure 1. Drawings of the Hull and the PTO System.

2.1 The Prototype
The 1:45 scale prototype of the inertial device has been designed and projected by ENEA and posteriorly tested in the wave channel of the Politecnico di Torino, using regular waves for different conditions of wave characteristic and control parameters of the PTO system [9]. The hull is made of stainless steel sheets of 1 mm thickness welded together. Two lateral fins facilitate the stabilization of the apparatus and its alignment respect to the direction of incident waves. At the bottom of the hull different masses are fixed, in order to balance the whole

structure and minimize instabilities, especially in roll. The masses are distributed between the two sides in such a way that they do not interfere with the movements of the pendulum. A frame is rigidly connected to the hull in order to support the load cell, the electric generator and the entire pendulum mechanism. A picture of the constructed prototype is shown in Fig. 2. The rest of the experimental setup is described in Appendix A.

Figure 2. Picture of the 1:45 Scale Prototype.

2.2 Lagrangian Model
In order to identify the characterizing parameters of the device a first model of the system has been built using a Lagrangian approach. For sake of simplicity it has been planned to construct the simplest possible mechanical analogy of the converter, ideally trying to represent the entire system with multi-body concentrated masses. For this purpose, and to adequately replicate the reaction to incident waves, a three-spring-damper system has been used, which acts in parallel with the three Cartesian axes of the reference system. Springs and dampers constrain the movements of the hull to displacements (horizontally and vertically) along the X-Y plane, and rotations around an axis perpendicular to this plane. Also the pendulum is constrained to oscillate in the X-Y plane. Therefore, in total 4 degrees of freedom are considered. Consequently the pursued variables are indicated as $(X_M, Y_M, \gamma, \theta)$ which represent respectively horizontal and vertical displacements of the hull, angular amplitude of the hull in pitch and angular amplitude of the pendulum. A scheme of the mechanical model adopted is shown in Fig. 3. Motion equations derived according to this approach are reported in Appendix B.

2.3 Model in SimMechanics
Numerical modelling is usually used to save time and money in the project development of a device, reducing risks related to design and planning operations and giving useful indications for later stages. Recently it has become a common practice also in Marine Energy sector [7], due to its multiple advantages over experimentation alone. In fact, often numerical modelling is the only way to facilitate multi-variable optimization of WECs in terms of performance, hydrodynamic loads, reaction loads and cost of energy produced. Normally, computational tools based on Computational Fluid Dynamics (CFD) and Finite Element Analysis (FEA) are used for such purposes [7–9]. However, these models are very complex

and their implementation is time consuming and requires large computational resources, which at the end translates to high economic costs [10–12].

Figure 3. Schematic Representation of the Mechanical Analogy studied with the Lagrangian Approach.

In this work a modelling tool has been developed which is characterized by accessibility to a wide range of users and exportability, which allows a fast and versatile modelling in order to obtain preliminary estimations on the performance and effectiveness of a new WEC design. This tool could be addressed to the category of hydrodynamic models, which are based on solving the force balance equations of motion, but differs from them because it is rather based on handling with mechanical analogies and the use of Matlab/Simulink/SimMechanics [13]. A scheme of the model implemented in SimMechanics environment is presented in Fig. 4. The final purpose of this approach is in fact to describe wave-device interactions using mechanical quantities, easier to treat and define than hydrodynamics matrices. The proposed approach allows the analysis of different constructive solutions and different operating conditions without losing simplicity required for a first approach in WEC modelling. Validity of such methodology has been already demonstrated in naval sector [14–17], but never before, as far as the authors know, for WEC characterization.

All the model parameters have been adjusted in an iterative process, with the final goal to obtain the best possible agreement between numerical and experimental results. In order to do that, some assumptions have been made on incident waves and geometry of the converter, as well as on their mutual interaction, with the aim to make them interact in a proper way that is representative of real interactions. Some of these impositions were assumed on the basis of manuals of naval architecture [17–19], papers and works of thesis about ship stabilization, control and optimization [14–17]; others have been added to give physical sense to the entire model. All the adopted assumptions and conventions are described in Appendix D.

3. RESULTS

In this section the results of experimental tests, numerical model and their comparison are presented. Finally, a study case is presented as an example of application of the implemented model.

Figure 4. Schematic Representation of the Simulink/SimMechanics model.

3.1 Experimental Results
The experimental tests were performed in Politecnico di Torino wave flume, not only to see the real behaviour of the prototype but also and especially to obtain reference values for the model to develop. During the tests, wave profile, motion of the hull and motion of the pendulum were analysed. Regular waves of constant height were used in a range of wave periods between 0.9 s and 1.4 s, in order to get a system response for different frequencies of the incident wave [9]. Test parameters and prototype configurations are summarized in Table 1, which contains all possible combinations of wave periods and damping coefficients which were examined.

Table 1. Values of test parameters and prototype configurations.

Parameter	Value
Wave Height H (crest to trough) (m)	0.05
Wave period T (s)	0.9 – 1.0 – 1.1 – 1.2 – 1.3 – 1.4
Pendulum length l (m)	0.334
Pendulum mass μ (kg)	3
Prototype mass M (kg)	75
PTO spring constant k (Nm/rad)	0
PTO damping constant b (Nms/rad)	0.1 – 0.3

The examined quantities were: angular amplitude of the hull in pitch γ, angular amplitude of the pendulum θ, extracted power P and Relative Capture Width (RCW). This last parameter expresses a sort of efficiency of the device, and it is defined as the ratio between the outgoing power from the PTO of the device (W) and the power density of the incident wave (W/m) multiplied by the

width of the hull (m). The graphs that show the experimental trends are illustrated in Appendix C. Looking at the graphs it is possible to make some preliminary considerations on the behaviour of the device [9]. Firstly, by increasing the damping coefficient of the PTO system the amplitude of oscillation of the pendulum decreases, and consequently also the relative velocity between hull and pendulum. This should lead to a decrease of the produced power. But with increased damping also the torque applied to the PTO increases. For this reason, there will exist an equilibrium for which the output power is maximized for a given damping coefficient, variable for each wave period. Thus, each wave will have an optimal damping coefficient to maximize the power absorption. This is a useful hint for future developments in terms of optimization and control of the device. Regarding the Relative Capture Width, it reaches values higher than 30% up to the maximum of about 45%, demonstrating good absorption capacity of the system, able to convert a significant percentage of the incident wave power.

3.2 Comparison of results from simulation and experiment

Once acquired all the information related to the behaviour of the device in wave tank, several simulations have been run with the model implemented in SimMechanics, trying to recreate wave flume conditions and examining the performance of the device in the same range of experimental tests. At the end, simulation results have been compared with the experimental results. This comparison is illustrated in Fig. 5 and Fig. 6. Continuous red lines indicate simulated trends, dashed black lines experimental trends. Empty markers indicate a damping coefficient of the PTO system of b = 0.1 Nms/rad, filled markers a damping coefficient b = 0.3 Nms/rad.

Several conclusions can be drawn from Fig. 5 and Fig. 6 regarding the goodness of the implemented model in SimMechanics. The model in fact seems to better predict the evolution of the oscillation amplitudes of the pendulum rather than those of the hull. Though, these two quantities are related to each other, since the pendulum displacement is considered respect to hull's reference frame, so a discrepancy in hull displacements is reflected also in pendulum discrepancies. However, for both the hull and the pendulum, major disagreements between the analytical model and experimental measurements are observed for periods of the incident wave between 1.2 s and 1.4 s, i.e. in proximity of the resonance period of the system (about 1.3 s). In the case of hull oscillations the two trends (and accordingly the absolute values of the amplitudes) disagree in the vicinity of the resonance period of the system, while in the case of the pendulum oscillation trends match but the model overestimates the experimental data. These overestimations produce an increase of the estimated power (and therefore of the RCW) compared to the experimental power output. Finally, qualitative and quantitative differences between the analytical model and the experimental one are almost similar for the two tested values of the damping

coefficient b of the pendulum (0.1 and 0.3 Nms/rad), while the trends of power and RCW better match for a damping coefficient of the pendulum of b = 0.3 Nms/rad.
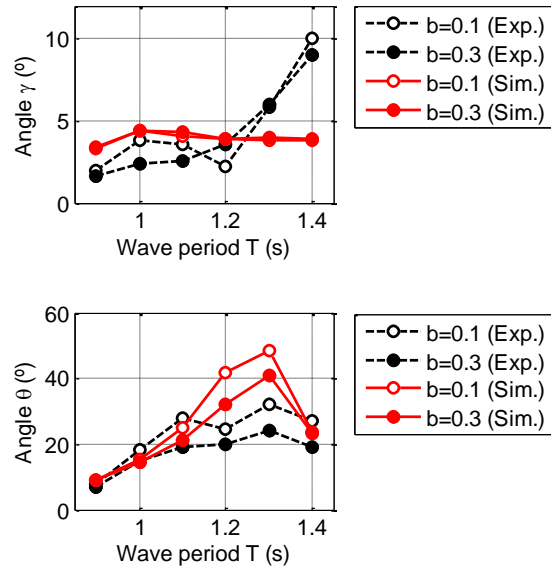

Figure 5. Comparison experimental-simulated trends. Hull's oscillations (above), pendulum oscillations (below).
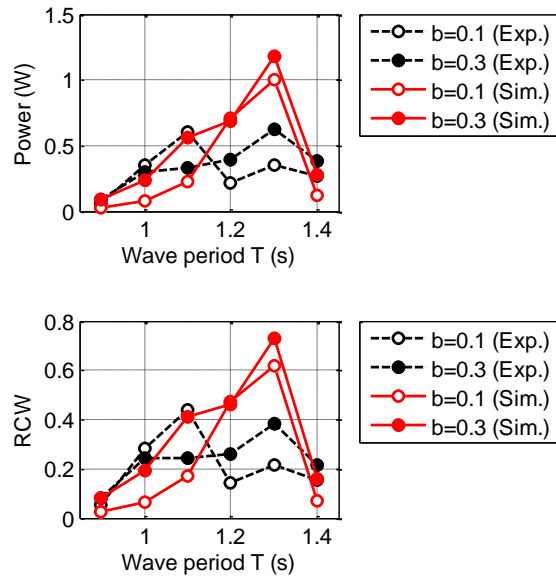

Figure 6. Comparison experimental-simulated trends. output power (above), RCW (below).

Then, in order to better analyse the deviations of the values forecasted by the model from the experimental ones, a deviations analysis with regard to the output power has been done for both values of the damping coefficient b of the pendulum. Deviations have been examined on the output power because for energy production assessments it is the most relevant parameter. The terms calculated to evaluate these deviations have been: *Absolute Error (AE), Mean Squared Error (MSE),*

Percentage Mean Squared Error (PMSE). As a "mean" value it has been used the reference value for the measurements, i.e. the experimental one. The results of the analysis are reported in Table 2 and Table 3. It can be observed how discrepancies vary significantly depending on the considered wave period and, as already anticipated by the related graphs, major disagreement occurs in the vicinity of the resonance period of the system.

However, when considered in absolute or relative terms, these changes are likely to be misleading, since it is recalled that the values analysed roam on the order of tenths (sometimes cents) of Watts, so slight variations of these values lead to considerable differences between the two models that do not reflect real dissimilarities. For the same reason, accuracy of measurements introduces another source of uncertainty. This reflects also the difficulty of scaling for PTO systems in WECs. However, if it is considered the PMSE, which is a risk function that indicates in percentage terms the discrepancy between the square values of the observed data and the values of the estimated data, it is observed how this remains quite low for all measures, and only in case of resonance it reaches 42% and 31% (for the two damping coefficients respectively).

Thus, discrepancies between the forecasts of the analytical model and the experimental results are considered acceptable within tolerances on simulations.

Table 2. Analysis of power deviations (W) for pendulum damping coefficient b = 0.1 Nms/rad.

T(s)	Simulated	Experimental	AE	MSE	PMSE
0.9	0.03	0.06	0.03	0.0009	0.09%
1.0	0.08	0.35	0.27	0.0729	7.29%
1.1	0.23	0.60	0.37	0.1369	13.69%
1.2	0.71	0.21	0.50	0.250	25.00%
1.3	1.00	0.35	0.65	0.4225	42.25%
1.4	0.12	0.27	0.15	0.0225	2.25%

Table 3. Analysis of power deviations (W) for pendulum damping coefficient b = 0.3 Nms/rad.

T(s)	Simulated	Experimental	AE	MSE	MSEP
0.9	0.09	0.09	0.00	0.000	0.00%
1.0	0.24	0.30	0.06	0.004	0.36%
1.1	0.56	0.33	0.23	0.053	5.29%
1.2	0.69	0.39	0.30	0.090	9.00%
1.3	1.18	0.62	0.56	0.314	31.36%
1.4	0.27	0.38	0.11	0.012	1.21%

3.3 Example of Application – Study Case for Energy Production Estimation

As an example of application of the developed model, a demonstration of energy production estimation has been carried out for two different locations in the Mediterranean Sea, for which the device was thought and projected from the beginning. The two chosen locations are Alghero and Lampedusa, quite well known in the oceanographic environment for being two of the most interesting sites in the Mediterranean Sea, in terms of wave power availability. For Alghero, energy production has been estimated for other WECs [5,20], thus results can be compared. These two places are represented with stars in Fig. 7. For the two locations wave data were available to the authors from 01/01/2001 to 31/12/2010 (10 years). Based on these data "Scatter Diagrams" were elaborated for both sites, representing the long-term probability of occurrence of sea states in terms of waves having certain height H and period T [2]. These two diagrams are represented in Appendix F. The objective of this exercise is to give a first idea of how much energy could be produced and if consequently it is worth further investigating on this kind of devices. In order to obtain an energy estimation from the scatter diagram, the power matrix of the device is needed [2,7], which gives the response of the device in terms of produced power for each sea state.
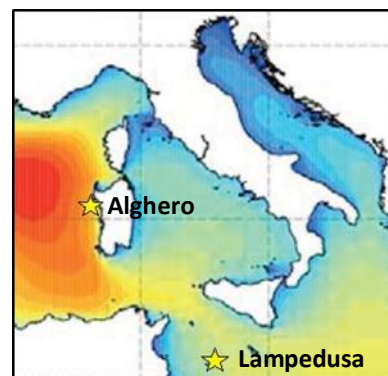

Figure 7. Representation of Alghero and Lampedusa within colour distribution of average wave power around Italy.

For generating the Power Matrix of the prototype, initially no control mechanisms or strategies in order to increase the energy absorption were implemented, neither any optimization of PTO parameters has been done. Moreover no rated power of the PTO or cut-in/cut-off working values of the same have been imposed. The power matrix without any limitations and considering regular waves, for the 1:45 prototype with pendulum damping coefficient of b = 0.1 Nms/rad, is shown in Appendix F (Fig. F.2). Once obtained the Power Matrix of the prototype it is possible to apply Froude Scaling Laws [20–22], listed in Appendix E, to obtain the corresponding Power Matrix for the full-scale device. Froude scaling has been adopted as it is commonly applied in physical WEC models [20]. Again, not only because any electrical/mechanical restrictions that limit the efficiency or the performance of the device have been applied, but also because it has been produced considering purely sinusoidal waves, the resulting Power Matrix for the full-scale device illustrated in Fig. 8 is to be considered purely theoretical. Then, in order to give more realistic values of energy produced by one device in

one year, other assumptions are needed. These have been chosen in order to obtain a sort of guaranteed least possible value, which means a conservative hypothesis of estimation.
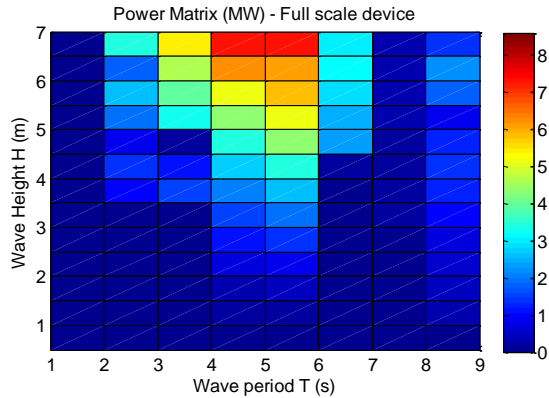

Figure 8. Theoretical Power matrix of the full scale device.

The assumptions made are:

- Rated power of the generator 100 kW;
- Minimum produced power of generator 10 kW;
- Power matrix values reduced by 30% (for possible overestimations of the model);
- Total operating time of the device reduced by six weeks a year (due to eventual breakages, maintenance operations and too powerful sea states when the device is turned off to preserve its integrity);
- Losses in the final production of 40% (30% due to electrical and mechanical losses in all the components of the PTO system, 5% electrical losses in cables, 5% losses in wave resource due to interactions with the bottom);
- No control on the device, and therefore optimization of the PTO, depending on the state of the sea.

The production values for one isolated device (so not considering losses due to WECs interactions in an eventual array) were 226 MWh/year in Alghero and 265 MWh/year in Lampedusa, which represents 25.8% and 30.3% of equivalent operation hours at nominal power (capacity factor).
These values seem to be still pretty optimistic for marine energy converters. For example, in [5,20] capacity factors between 15-20% were reported for Alghero site.
However, this example is useful to illustrate what can be done with a modelling tool like the one implemented in this work, i.e. make preliminary assessments to verify the effectiveness of a certain device. When considering real irregular waves these values will certainly decrease, but still they can give good indications for the prospective of the device.

4. LIMITATIONS AND FUTURE GUIDELINES

In this work the best possible compromise between model accuracy and simplicity of the same has been pursued. For this reason it has been decided to use a purely mechanical analogy, which allowed avoiding the hydrodynamic characterization of the hull and the effects of added mass and radiation waves, and consequently the specialized software required for such purposes. Obviously this methodology is affected by some assumptions and limitations, both on wave and device geometry, which restrict its validity as unique required tool for this kind of characterizations. For instance, modelling of the incident waves leads to an idealization of the phenomena in wave-device interactions. Moreover, the spring-damper analogy may miss some of the aspects that describe the complete behaviour of a floating body, e.g. the coupling terms between different DOFs. Finally, some of the hull's parameters have been considered constant during the entire simulation, which is a valid approximation only for relatively small movements or oscillations.
As future guidelines, the model could be adjusted using an adequate tuning procedure (e.g. least squares method) or a more sophisticated optimization algorithm. Also initial parameterizations could be improved, assigning inertia values and geometries directly calculated trough CAD software or further refining the values of elastic and damping constants. Finally, the limit of having used regular sinusoidal forces could be removed introducing wave component parameters in order to reproduce a more realistic sea state. On the other hand, improvements could come from the experimental point of view, for instance modifying the actual test layout through a wireless control system (*telemetry*) avoiding the influence of signal cables on system dynamics. Repeating the test in a deeper wave tank would reduce interactions of the system with the bottom. And finally, extending tests to other wave conditions, different PTO control and configurations of the prototype would help to adjust and validate the model in a broader range of conditions.

5. CONCLUSIONS

This work has been focused on the modelling of a passive inertial WEC, motivated by the need of developing a simple, user friendly and versatile design tool. This tool is designed for making preliminary assessments of general nature about goodness and performance of different types of Wave Energy Converters. According to such requirements several assumptions have been made in order to take into account all relevant aspects of wave-device interactions.
The results of the experimental test campaign on a 1:45 scaled prototype were the basis for the numerical model implementation, simulating the dynamics of the system and analysing the produced power. Despite the adopted simplified approach, numerical estimates show a good agreement with real trends. Nevertheless, there is still

room for substantial improvements. With further investigation and more sophisticated tuning procedures this methodology can be improved, increasing its usefulness in WECs modelling and development.

Finally, as an example of application, energy estimations have been made for two different locations in the Mediterranean Sea. Using a conservative hypothesis, projections have confirmed that the investigated technology is auspiciously promising and worth to be further investigated and implemented. This confirms also that Inertial WECs are an interesting option for energy supply from renewable sources.

6. REFERENCES

[1] O. Langhamer, K. Haikonen, J. Sundberg, Wave power-Sustainable energy or environmentally costly? A review with special emphasis on linear wave energy converters, Renew. Sustain. Energy Rev. 14 (2010) 1329–1335. doi:10.1016/j.rser.2009.11.016.

[2] A.F. de O. Falcão, Modelling of wave energy converters, Instituto Superior Tecnico, Lisboa, 2014.

[3] J. Falnes, Ocean Waves and Oscillating Systems: Linear Interactions Including Wave-Energy Extraction, Cambridge University Press, Cambridge, 2002.

[4] G. Bracco, E. Giorcelli, G. Mattiazzo, E. Tedeschi, M. Molinas, Control Strategies for the ISWEC Wave Energy System, in: 9th Eur. Wave Tidal Energy Conf., 2011.

[5] S. Bozzi, A.M. Miquel, A. Antonini, G. Passoni, R. Archetti, Modeling of a point absorber for energy conversion in Italian seas, Energies. 6 (2013) 3033–3051. doi:10.3390/en6063033.

[6] M. Ruellan, H. Benahmed, B. Multon, C. Josset, A. Babarit, A. Clement, Design methodology for a SEAREV wave energy converter, IEEE Trans. Energy Convers. 25 (2010) 760–767. doi:10.1109/TEC.2010.2046808.

[7] P. Ruiz-Minguela, Progress in the development of OCEANTEC wave energy converter, in: 3rd Int. Symp. Ocean Energy, Bilbao, 2009.

[8] A.P. McCabe, A. Bradshaw, J.A.C. Meadowcroft, G. Aggidis, Developments in the design of the PS Frog Mk 5 wave energy converter, Renew. Energy. 31 (2006) 141–151. doi:10.1016/j.renene.2005.08.013.

[9] G. Mattiazzo, E. Giorcelli, G. Bracco, E. Giovannini, A. Fontanella, Sintesi delle attività di sviluppo di un dispositivo inerziale passivo per la produzione di energia dal moto ondoso, ENEA Report 172, 2013. http://www.enea.it/it/Ricerca_sviluppo/documenti/ricerca-di-sistema-elettrico/energia-dal-mare/2013/rds-par2013-172.pdf.

[10] M. Folley, A. Babarit, B. Child, D. Forehand, L. O'Boyle, K. Silverthorne, et al., A Review of Numerical Modelling of Wave Energy Converter Arrays, Vol. 7 Ocean Sp. Util. Ocean Renew. Energy. (2012) 535–545. doi:10.1115/OMAE2012-83807.

[11] M.K. Tautra Hoen, Modelling and Control of wave energy converters, Norwegian University of Science and Technology, 2009. http://www.diva-portal.org/smash/get/diva2:347732/FULLTEXT01.pdf.

[12] B.W. Nam, S.Y. Hong, J. Park, S.H. Shin, S.W. Hong, K.B. Kim, Performance Evaluation of the Floating Pendulum Wave Energy Converter in Regular and Irregular Waves, Int. J. Offshore Polar Eng. 24 (2014) 45–51.

[13] The MathWorks, Multibody Simulation - SimMechanics, (2015). http://www.mathworks.com/products/simmechanics/ (accessed October 1, 2015).

[14] J.L. Doblack, Modelling and control for the reduction of wave induced motion of ramp-connected ships, Univertity of California, San Diego, 2011. https://escholarship.org.

[15] J. Toubi, Control and optimization of wave-induced motion of ramp- interconnected craft for cargo transfer, Univertity of California, San Diego, 2009. https://escholarship.org.

[16] S.H. Oonk, Wave-induced motion of ramp-interconnected craft, Univertity of California, San Diego, 2008. https://escholarship.org.

[17] A. Biran, R. López-Pulido, Chapter 6 - Simple Models of Stability, in: Sh. Hydrostatics Stab., Butterworth-Heinemann, Oxford, 2014: pp. 127–169. doi:http://dx.doi.org/10.1016/B978-0-08-098287-8.00006-2.

[18] T. Miloh, Maneuvering Hydrodynamics of Ellipsoidal Forms, Schriftenr. Schiffbau. 357 (1977). doi:10.15480/882.677.

[19] E. Pesman, D. Bayraktar, M. Taylan, Influence of damping on the roll motion of ships, in: 2nd Int. Conf. …, 2007: pp. 127–134. http://web.itu.edu.tr/~pesman/Paper_ICMRT07.pdf.

[20] S. Bozzi, R. Archetti, G. Passoni, Wave electricity production in Italian offshore: A preliminary investigation, Renew. Energy. 62 (2014) 407–416. doi:10.1016/j.renene.2013.07.030.

[21] J.F. Langan, Chapter 4 - The Continuity Equation, the Reynolds Number, the Froude Number, in: An Introd. to Aerodyn., 1988. http://www.yale.edu/ynhti/curriculum/units/1988/6/88.06.04.x.html.

[22] V. Ruggiero, Appunti del corso di architettura navale, Università degli studi di Messina, 2008. http://ww2.unime.it/ingegneria/new/materiale/APPUNTI DEL CORSO DI ARCHITETTURA NAVALE-6dic08.pdf.

[23] G. Mattiazzo, E. Giorcelli, D. Poggi, Valutazione della produttività di sistemi attivi su struttura galleggiante per la generazione di energia da moto ondoso, ENEA Report 173, 2012. http://openarchive.enea.it//handle/10840/4528.

[24] G. Bracco, E. Giorcelli, G. Mattiazzo, ISWEC: Design of a Prototype Model for Wave Tank Test, in: 10th Bienn. Conf. Eng. Syst. Des. Anal., Istanbul, 2010: pp. 25–31. doi:10.1115/ESDA2010-24120.

APPENDICES

A. EXPERIMENTAL SETUP

Experimental tests were carried out in the wave tank of Politecnico di Torino. This channel is 50.4 m long and 0.6 m deep, but the water depth can be varied. At one end of the channel a wave maker is installed. The wave propagates through the channel and reaches the prototype; part of the wave continues over the prototype up to arrive at the opposite end of the channel where a wave absorber dissipates its energy [9]. Even if the device floats by itself, it needs a mooring system to not being taken adrift by waves and currents. To accomplish this task four equidistant holes were placed in angular direction on lateral fins on the bottom of the hull. Through these holes a mooring chain can be connected to a mass resting on the bottom of the channel and passing by a floater. Besides, polyurethane foam blocks have been added to the lateral rod nuts, in order to not damage the testing channel. Pictures of the prototype in the wave flume and its mooring system are illustrated in Fig. A.1.
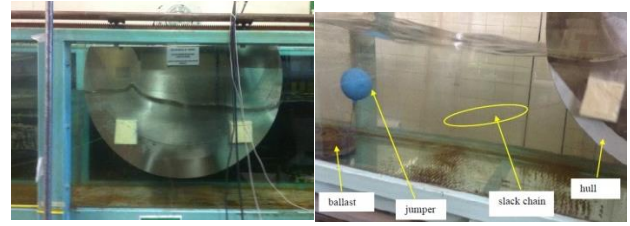

Figure A.1. Prototype in the wave flume and its mooring system

B. LAGRANGIAN FORMALISM

Subsequently the mathematical formulation adopted to describe the system with the Lagrangian approach is presented.

Mass M (Hull): Position and Velocity

$$\begin{cases} X_M \\ Y_M \end{cases} ; \quad \begin{cases} \dot{X}_M \\ \dot{Y}_M \end{cases}$$

Mass μ (Pendulum support): Position and Velocity

$$\begin{cases} X_\mu = X_M + L\sin\gamma \\ Y_\mu = Y_M + L\cos\gamma \end{cases} ; \quad \begin{cases} \dot{X}_\mu = \dot{X}_M + L\dot{\gamma}\cos\gamma \\ \dot{Y}_\mu = \dot{Y}_M - L\dot{\gamma}\sin\gamma \end{cases}$$

Mass m (Mass of the pendulum): Position and Velocity

$$\begin{cases} X_m = X_\mu + l\sin\theta \\ Y_m = Y_\mu + l\cos\theta \end{cases} ;$$

$$\begin{cases} \dot{X}_m = \dot{X}_M + L\dot{\gamma}\cos\gamma + l\dot{\theta}\cos\theta \\ \dot{Y}_m = \dot{Y}_M - L\dot{\gamma}\sin\gamma - l\dot{\theta}\sin\theta \end{cases}$$

Kinetic energy T, Potential energy U and Dissipative Term P:

$$T = \frac{1}{2}\sum_i m_i \dot{r}_i^2 = \frac{1}{2}M\left(\dot{X}_M^2 + \dot{Y}_M^2\right) + \frac{1}{2}\mu\left(\dot{X}_\mu^2 + \dot{Y}_\mu^2\right)$$
$$+ \frac{1}{2}m\left(\dot{X}_m^2 + \dot{Y}_m^2\right) + \frac{1}{2}I_\mu\dot{\gamma}^2 + \frac{1}{2}I_m\dot{\theta}^2 \tag{1}$$

$$U = \sum_i m_i g Y_i + \frac{1}{2}\sum_i K_i r_i^2$$
$$= MgY_M + \mu gY_\mu + mgY_m + \frac{1}{2}K_1 X_M^2$$
$$+ \frac{1}{2}K_2 Y_M^2 + \frac{1}{2}K_3\gamma^2 \tag{2}$$

$$P = \frac{1}{2}\sum_i B_i \dot{r}_i^2 = \frac{1}{2}B_1\dot{X}_M^2 + \frac{1}{2}B_2\dot{Y}_M^2 + \frac{1}{2}B_3\dot{\gamma}^2 \tag{3}$$

These quantities are connected to each other by the *Euler–Lagrange equation*:

$$\frac{d}{dt}\frac{\partial L}{\partial \dot{q}} - \frac{\partial L}{\partial q} + \frac{\partial P}{\partial \dot{q}} = \sum F_{ext} \tag{4}$$

Where L is the *Lagrangian* of the system and is given by

$$L = T - U \qquad (5)$$

Executing substitutions and differentiations it can be obtained a system of four differential equations which describe the behaviour of the system.

C. EXPERIMENTAL TRENDS

Graphs illustrating results of the experimental tests alone are reported in Fig. C.1 and Fig. C.2. Empty markers indicate a damping coefficient of the PTO system of b = 0.1 Nms/rad, filled markers indicate b = 0.3 Nms/rad.
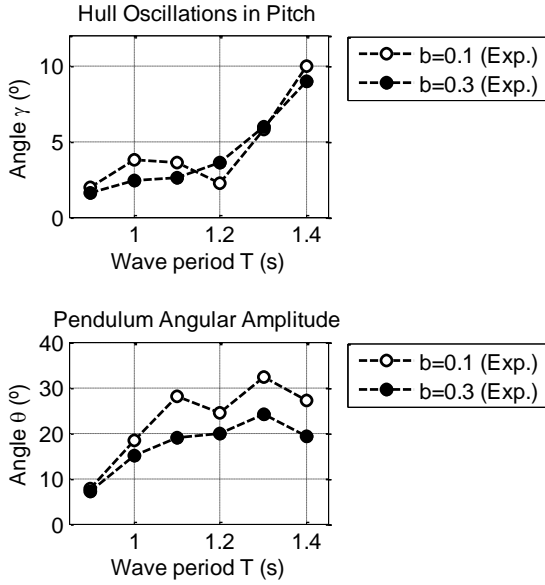

Figure C.1. Experimental trends of oscillations of hull (above) and pendulum (below).
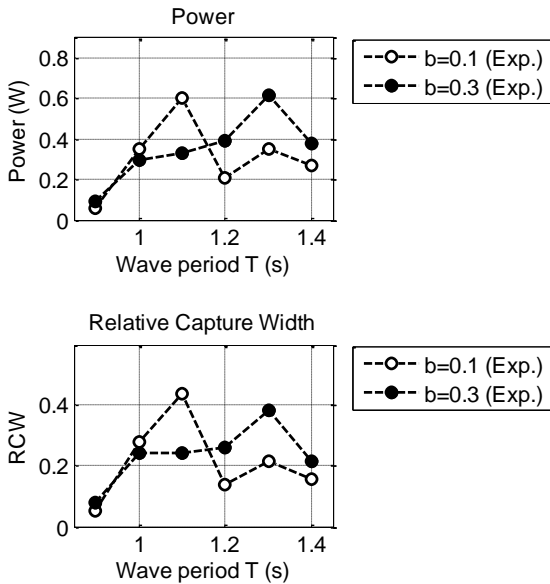
Figure C.2. Experimental trends of Power (W) (above) and Relative Capture Width (below).

D. MODEL ASSUMPTIONS

About hull geometry, it has been assumed that it can be modeled as a half-cylindrical shell, empty inside, which is a reasonably good approximation considering the likeness with the real shape. It is submerged for half of its height, which is an assumption made on the basis of empirical observations on the prototype in wave tank, Three spring-damper systems are connected to strategic locations of the hull: one at the center of gravity and two in correspondence of water line to simulate gravity-buoyancy actions. Vertical forces representing the waves act upwards in two points in correspondence of the waterline and of the points in which have been applied the spring-damper systems, at half height and half width of the hull, in order to simulate the approaching waterfront. These assumptions are resumed and represented in Fig. D.1. The mass and inertia properties, which proved to be particularly important for this type of modelling, were calculated using geometric relationships or, wherever possible, taken directly from the values calculated with CAD software.

Table 4. Simulation assumptions and chosen values.

Quantity	Assumed Value
Gravity	mg
Buoyancy	$\rho g V$
F_{wave}	$\rho g A_W \zeta$
Phase shift	$\dfrac{2\pi L}{\lambda}$
Wavelength	$\left(\dfrac{gT^2}{2\pi}\right)\left\{\tanh\left[2\pi\sqrt{\dfrac{(d/g)}{T}}\right]^{3/2}\right\}^{2/3}$
k_{surge}	10000 N/m
k_{heave}	$\rho g A_W$
k_{pitch}	$m_{device}\, g\, \overline{GM}$
b	$0.01\ Nms/rad$
b_{surge}	$2b$
b_{heave}	b
b_{pitch}	$2\, b\, m_{device}\left(\dfrac{L}{2\sqrt{3}}\right)^2$

Regarding the incident waves, these were modelled in linear wave theory [2,3,14] as sinusoidal forces whose intensity is proportional to wave height and waterplane area of the hull, in such a way to facilitate their implementation in Matlab/SimMechanics environment. Amplitude, wavelength, and phase of the two harmonic components have been obtained from the only known data of the generated waves in wave tank during experimental tests, i.e. period and amplitude. Assumed values for the remaining wave properties are reported in

Table 4. Phase shift between wave components was established on the basis of the intuitive observation that for a length of the hull equal to the wavelength of the incident wave different waterfronts will meet hull's extremities at the same time. That concept is extendible to all the situations in which the hull's length is multiple of the wavelength, as ideally represented in Fig. D.1.

With regard to implemented spring-damper coefficients, their values were calculated in different ways. Elastic constants were deduced from the respective equation of motion for the single degree of freedom considered for Heave (5) and Pitch (6), hereinafter presented [14–16].

$$(m + A_\omega)\ddot{x} + b\dot{x} + (\rho g A_W)x = F\cos(\omega t) \qquad (5)$$

$$J\ddot{\gamma} + (2Jb)\dot{\gamma} + (g\, m_{device}\, \overline{GM})\gamma = F\sin(\omega t) \qquad (6)$$

In surge there are no hydrostatic restoring forces; components in this DOF represent only the action of moorings, so spring constant in this case was arbitrarily assumed in order to give physical sense to the resulting motion of the hull in surge, on the basis of experimental observations during tests. The same reasoning has been made for damping coefficients in surge and heave, since no proper formula has been found for these elements. Instead, in pitch, damping coefficient has been directly related to length and mass of the device through the so-called "mass radius of gyration" ($L/2\sqrt{3}$) about the axis of inclination for pitch motion and for half-cylinder geometry.
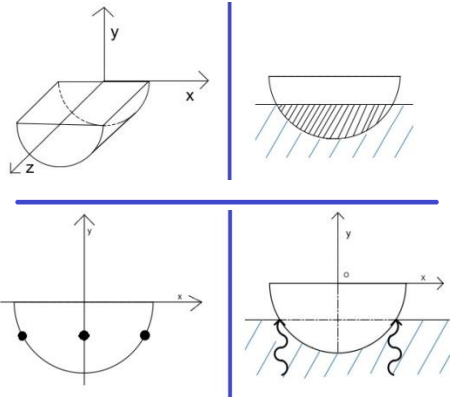

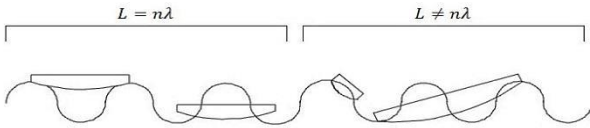Figure D.1. Hull's Geometry Modelling and Assumptions.

Figure D.2. Representation of the Consideration made to establish Wave Forces Phase Shift.

E. FROUDE SCALING

In hydrodynamic characterization problems, the three fundamental forces to take into account are the inertial forces, the force of gravity and the viscous forces. There are two expressions that make allowance for the relative importance of these forces, respectively called *Reynolds number* and *Froude number,* and whose expression is given by:

$$Fr \propto \frac{inertial\ forces}{gravitational\ forces} = \frac{V}{\sqrt{gl}}$$

and

$$Re \propto \frac{inertial\ forces}{viscous\ forces} = \frac{Vl}{\nu}$$

Where V is the velocity of the fluid, l the considered length, g the gravitational constant and ν the kinematic viscosity. In determining the scaling parameters to pass from the scaled to the full-scale model, the ideal would be to maintain the balance and proportions between these forces, while keeping unchanged both the Reynolds number and the Froude number. In practice, however, both conditions are difficult to obtain, since this would imply a change in gravitational acceleration or in kinematic viscosity. Therefore, under the consideration that in these tests gravitational forces are predominant compared to viscous forces, it is common to use scaling relations that preserve the Froude number. The relationships to be used in Froude scaling are indicated in the following table, in which *s* indicates the scale of the prototype used for the tests. Multiplying each of the test results or data for the related quantity, the corresponding value in the full scale model is obtained. Froude scaling laws for different parameters are reported in Table 5.

Table 5. Froude scaling laws for various quantities; s is the geometric scale value.

Quantity	Scaling factor
Wave Height	s
Wavelength	s
Wave Period	$s^{0,5}$
Wave Frequency	$s^{-0,5}$
Power Density	$s^{2,5}$
Linear Displacement	s
Angular Displacement	1
Linear Velocity	$s^{0,5}$
Angular Velocity	$s^{-0,5}$
Linear Acceleration	1
Angular Acceleration	s^{-1}
Mass	s^{3}
Force	s^{3}
Torque	s^{4}
Power	$s^{3,5}$
Linear Stiffness	s^{2}
Angular Stiffness	s^{4}
Linear Damping	$s^{2,5}$
Angular Damping	$s^{4,5}$

F. SCATTER DIAGRAMS AND POWER MATRICES

In Fig. F.1 the scatter diagrams are presented for the two selected locations, Alghero and Lampedusa, representing the probability of occurrence of sea-states in terms of waves having certain height and period [2]. Wave data were collected from 01/01/2001 to 31/12/2010 (10 years). In order to compare these values with those implemented in the power matrix using regular waves, both scatter diagrams were produced using the average period T (in seconds) and the height H (in meters) of the regular wave equivalent to the real sea state. This last is obtained by imposing that the regular wave (H, T_e) and the real sea state (H_s, T_e) are isoenergetic [23,24]:

$$P_{reg} = \frac{\rho g^2}{32\pi} H^2 T_e \left[\frac{W}{m}\right] \cong H^2 T_e \left[\frac{kW}{m}\right] \tag{7}$$

$$P_{irreg} = \frac{\rho g^2}{64\pi} H_s^2 T_e \left[\frac{W}{m}\right] \cong H_s^2 T_e \left[\frac{kW}{m}\right] \tag{8}$$

$$P_{reg} = P_{irreg} \Rightarrow H^2 T_e = \frac{H_s^2 T_e}{2} \Rightarrow H = \frac{H_s}{\sqrt{2}} \tag{9}$$

In Fig. F.2 the Power Matrix recreated with the implemented model for the 1:45 scale prototype is presented as a function of H and T. In Fig. 8 was previously illustrated the same Power Matrix but for the full scale model, scaled with Froude Scaling Laws [21,22]. Please note that the resultant Power Matrix is to be considered purely theoretical, then unrealistic. In fact, in this preliminary stage of the study no electrical/mechanical limitations, assumptions and constraints of any kind have been applied in producing it. Besides, as already mentioned, the values of power produced were obtained using regular waves.
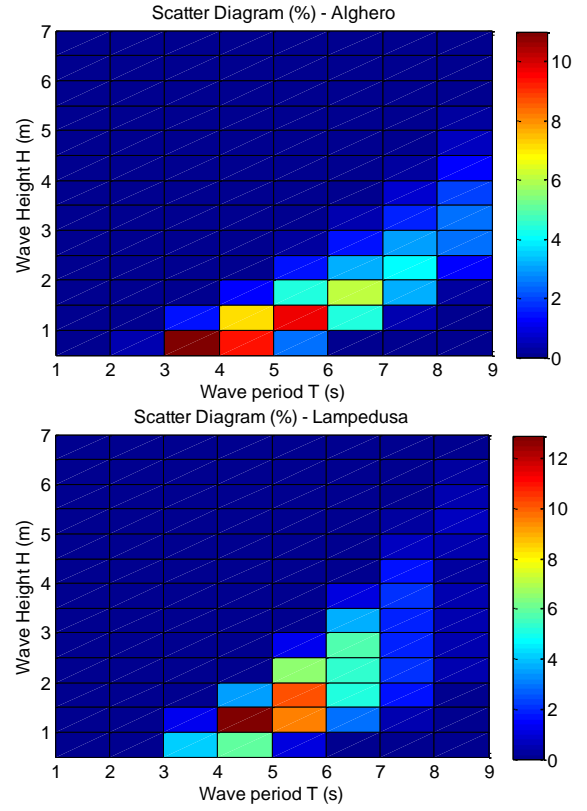

Figure F.1. Scatter Diagrams for Alghero (above) and Lampedusa (below) within colour distribution of wave probability of occurrence.
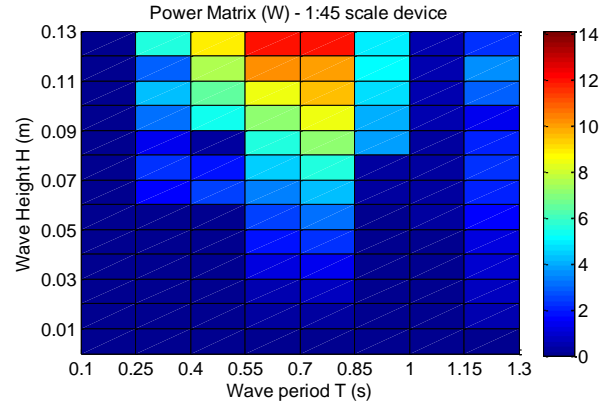

Figure F.2. Power matrix of the 1:45 scaled device.

11